New Parametric Scattering in Photorefractive $Sr_{0.61}Ba_{0.39}Nb_2O_6$:Cr

M. Goulkov and O. Shinkarenko

Institute of Physics, Science Avenue 46, 03650, Kiev-39, Ukraine

L. Ivleva and P. Lykov

Institute of General Physics, Vavilov Street 38, 119991, Moscow, Russia

T. Granzow and Th. Woike

Institute of Mineralogy, University of Cologne, Zülpicherstrasse 49b, D-50674 Cologne, Germany

M. Imlau and M. Wöhlecke

Department of Physics, University Osnabrück, Barbarastrasse 7, D-49069 Osnabrück, Germany

A new class of light-induced parametric scattering, not included in the conventional model, has been discovered in photorefractive $Sr_{0.61}Ba_{0.39}Nb_2O_6$:Cr illuminated by two coherent beams. A novel model of multiwave mixing of coherent noise and transmitted light is developed to explain the new scattering phenomena. The model includes all known types and predicts a multitude of new types of parametric scattering. Generalized phase-matching conditions for parametric scattering in photorefractive crystals are proposed.

Parametric light-induced scattering is a result of nonlinear amplification of coherent noise via four-wave-mixing (4WM) at the expense of the incident laser beams and is a general effect for optical materials with different types of nonlinearity. Up to now it has been reported in sodium vapours [1], dye solutions [2], molecular crystals [3], nematic liquid crystals [4], and photorefractive crystals [5], where it manifests itself in a rich variety of specific light patterns on the viewing screen behind a crystal. Especially high gain coefficients of 4WM (up to 100 cm^{-1}) found in photorefractive crystals allow to observe effective parametric scattering in these materials even with low power lasers. Seed and pump waves record noisy refractive index gratings via the photorefractive effect [6]: a nonuniform photoexcitation of electric charge carriers, caused by the exposure to a light interference pattern, results in the buildup of space charge fields modulating the refractive index via the linear electrooptic effect. These waves are simultaneously diffracted from the recorded gratings. In directions where light waves and recorded gratings obey certain phase-matching conditions, a dynamic feedback of the recording and readout processes will cause an amplification of the seed waves. Therefore, parametric scattering is a useful tool to study 4WM phenomena. The latter are especially important for applications of photorefractive crystals in optical image processing systems. It has been proposed to use processes of parametric amplification of scattered light for optical image amplification [7] and optical broadcasting [8]. On the other hand, in some cases, such as optical data storage, it is important to avoid light-induced scattering, a task which is difficult due to time dependent development of the scattering. The knowledge of the fundamental processes resulting in parametric scattering will probably allow the elimination or at least minimization of its effect. At the same time, light-induced scattering contains information about various material parameters, and, thereby, is an effective tool for contactless material characterization [9]. The intensity distribution in a parametric scattering pattern should give information on the particular mechanism of the optical nonlinearity [10].

The conventional model of parametric scattering distinguishes A- and B-type 4WM scattering processes described by phase-matching conditions [5]:

$$A\text{-type:} \quad \mathbf{k}_\alpha + \mathbf{k}_\beta = \mathbf{k}_\gamma + \mathbf{k}_\delta, \quad (1)$$

$$B\text{-type:} \quad \mathbf{k}_\alpha - \mathbf{k}_\beta = \mathbf{k}_\delta - \mathbf{k}_\gamma, \quad (2)$$

These conditions parametrically couple wave vectors of four waves, i.e., the scattered waves γ and δ and the pump waves α and β. According to Eqs. (1) and (2), the gratings $\mathbf{K}_s = \mathbf{k}_\gamma - \mathbf{k}_\beta$ and $\mathbf{K}'_s = \mathbf{k}_\alpha - \mathbf{k}_\delta$ recorded by the pairs γ-β and δ-α are identical: $\mathbf{K}_s = \pm\mathbf{K}'_s$. Therefore, diffraction of the pump wave α at the *alien* grating $\mathbf{K}_s$ yields the seed wave δ, and then its *own* grating $\mathbf{K}'_s$ is recorded. Analogously, diffraction of the pump wave β on the grating $\mathbf{K}'_s$ results in the seed wave γ and in recording of the grating $\mathbf{K}_s$. Enhancement of the gratings leads to increasing intensities of the waves γ and δ. In its turn, enhancement of these scattering waves further increases the amplitudes of the gratings $\mathbf{K}_s$ and $\mathbf{K}'_s$. Processes of parametric amplification will continue until the scattering reaches its steady state. In the general case, waves in Eqs. (1) and (2) may have different spatial orientation and polarization, and participate in different variants of

4WM. A geometry with two noncollinear laser beams is most convenient for studying parametric scattering. Waves amplified by A or B processes form cones oriented parallelly (A) or perpendicularly (B) to the bisector of the angle $2\theta_p$ between the pump beams and, respectively, result in rings or lines on the viewing screen. The equality of $\mathbf{K}_s$ and $\mathbf{K}'_s$ is a necessary condition for effective amplification in the conventional 4WM model. Thus, Eqs. (1) and (2) impose a strong restriction for possible variants of 4WM, allowing only 19 independent processes. However, not much attention has been given to the gratings $\mathbf{K}_f = \mathbf{k}_\alpha - \mathbf{k}_\beta$ and $\mathbf{K}'_f = \mathbf{k}_\delta - \mathbf{k}_\gamma$ in the common theoretical concept.

In the present Letter, we report on a new class of parametric scattering observed in photorefractive $Sr_{0.61}Ba_{0.39}Nb_2O_6$:Cr (SBN:Cr), which cannot be explained by the classic model of parametric scattering. We develop a novel 4WM model and apply it to the observed scattering. The mixing of coherent optical noise and pump waves is traced to various combinations of the fundamental grating $\mathbf{K}_f$ and noisy gratings. Inclusion of the grating $\mathbf{K}_f$ in the phase-matching conditions lifts the symmetry restrictions obvious from Eqs. (1) and (2) allowing for a great variety of new multiwave processes. Unified phase-matching conditions covering all known types of parametric scattering are proposed.

We used a photorefractive SBN single crystal doped with 0.02 wt% Cr_2O_3 grown by the modified Stepanov technique [11], cut with a thickness $l = 6.1$ mm along the a axis, and poled with an external electric field. Unexpanded α and β beams from an Ar-ion laser ($\lambda = 488$ nm) with equal intensities $I_p = 500$ mW/cm^2 impinged symmetrically upon the crystal, so that the polar $\mathbf{c}$ axis was oriented from β to α. The beams were marked by black disks on the viewing screen. For extraordinarily polarized beams, the scattering pattern consists of two series of lines of extraordinarily polarized light: line γ_1, γ_2, γ_3 on the right-hand side of beam β, and line δ_1, δ_2 on the left-hand side of beam α [see Fig. 1(a)]. The scattering intensity decreases with the line number, and γ lines are much stronger than δ lines. The total number of scattering lines decreases with increasing θ_p: lines with larger numbers vanish first. At $\theta_p = 7°$, only lines γ_1 and δ_1 remain detectable, as it is shown in Fig. 1(b). Besides the pump beams, an additional signal beam (also marked by a black disk on the photo) was directed through the crystal onto line γ_1. The new scattering spot symmetrically appearing on line δ_1 defines the fourth wave δ involved in the mixing process with waves γ, α, and β. The angular position of the scattering lines depends on the pump angle. Scattering angles θ_s measured in the plane of incidence from the normal on the crystal surface towards the direction of the scattering line are positive for γ lines and negative for δ lines. The dependence of θ_s on θ_p for lines induced by extraordinary beams is shown in Fig. 2 by unfilled marks. If the polar-
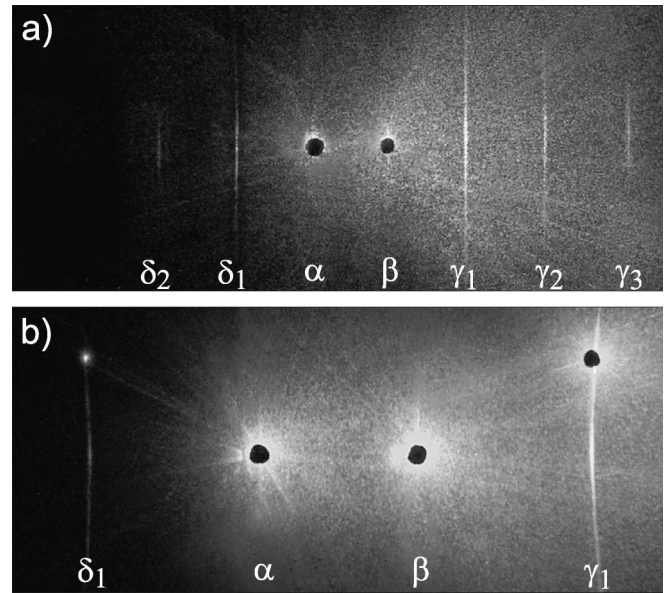

FIG. 1. Scattering patterns from two extraordinary pump beams observed on the viewing screen placed behind the crystal: (a) $\theta_p = 2.5°$, (b) $\theta_p = 7°$.

ization of the pump beams is changed to ordinary, the scattering also changes its polarization, but becomes much weaker: even for small angles θ_p only lines δ_1 and γ_1 were observed in the experiment. The scattering angle θ_s for ordinarily polarized light is shown versus θ_p in Fig. 2 by filled marks. These data can neither be explained by phase-matching conditions Eqs. (1) and (2), nor classified by the classic 4WM model of parametric scattering. According to [5], cones of polarization-isotropic scattering always touch the pump beams, so that $\theta_s = \theta_p$. Another peculiarity of the new scattering is the strong correlation between the scattering efficiency and the strength of the fundamental grating $\mathbf{K}_f$. Figure 3
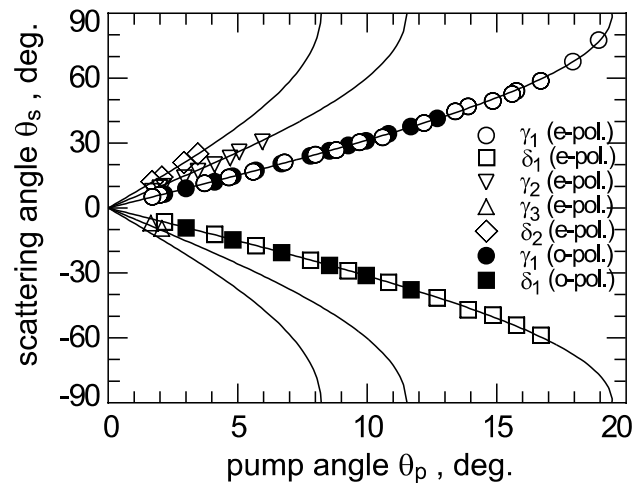

FIG. 2. Scattering angle θ_s versus pump angle θ_p for scattering lines γ_i and δ_i from extraordinary and ordinary pump beams.
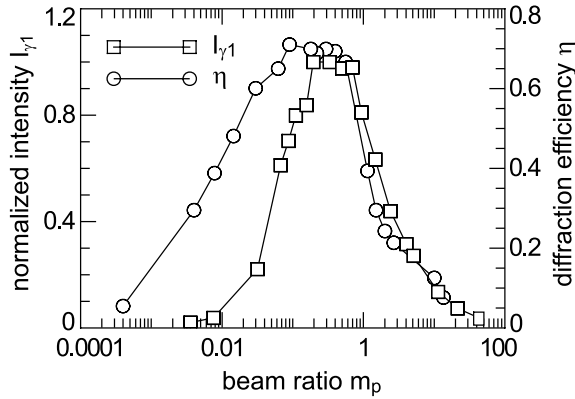
FIG. 3. Intensity of the scattering line γ_1 and diffraction efficiency of the fundamental grating $\mathbf{K}_f$ versus pump ratio m_p.

shows the intensity of line γ_1 shown in Fig. 1(b) and the diffraction efficiency η of the grating $\mathbf{K}_f$ measured versus the pump ratio $m_p = I_\beta/I_\alpha$. Note that the lines are not a result of scattering of higher orders of diffraction of the pump beams, since such high orders were not observed in the experiment.

We explain the scattering by the following model of 4WM of scattered and pump waves. Figure 4(a) shows wave vectors of two pump waves α and β, and two symmetric sets of scattering waves γ_j and δ_j (up to $j = 3$) in the plane of incidence. The waves γ_j and β record gratings $\mathbf{K}_{sj} = \mathbf{k}_{\gamma j} - \mathbf{k}_\beta$, and likewise the waves δ_j and α record gratings $\mathbf{K}'_{sj} = \mathbf{k}_\alpha - \mathbf{k}_{\delta j}$. Unlike the case described by Eq. (2), $\mathbf{K}_{sj}$ and $\mathbf{K}'_{sj}$ are not equal,

as shown on a larger scale for $j = 1$ in Fig. 4(b). However, $\mathbf{K}_{s1}$ can be considered as a combination of $2\mathbf{K}_f$ and $\mathbf{K}'_{s1}$, and vice versa. This will provide their parametric enhancement and increasing amplitudes of γ_1 and δ_1 by successive diffractions of wave α on gratings $2\mathbf{K}_f$ and $\mathbf{K}_{s1}$, and wave β on gratings $2\mathbf{K}_f$ and $\mathbf{K}'_{s1}$. The same process ($j = 1$) is shown in Fig. 4(c) on the viewing screen: the location of the waves γ_1 and δ_1 correlates with the scattering pattern in Fig. 1(b). 4WM for an arbitrary index j is described by the phase-matching conditions written in terms of grating vectors:

$$\mathbf{K}_{sj} + 2j\mathbf{K}_f = \mathbf{K}'_{sj}. \qquad (3)$$

An accounting of $\mathbf{K}_f$ considerably extends the possible variants of parametric mixing, and some of those, resulting in the same sets of scattering lines as above, are shown in Fig. 5. In Fig. 5(a), gratings $\mathbf{K}_{sj} = \mathbf{k}_{\gamma j} - \mathbf{k}_\beta$ and $\mathbf{K}_{dj} = \mathbf{k}_{\delta j} - \mathbf{k}_\beta$ satisfy the phase-matching conditions:

$$\mathbf{K}_{sj} + (2j + 1)\mathbf{K}_f = \mathbf{K}_{dj}. \qquad (4)$$

4WM by the gratings $\mathbf{K}_{dj}$ and $\mathbf{K}_{pj} = \mathbf{k}_{\gamma j} - \mathbf{k}_\alpha$ shown in Fig. 5(b) is described by:

$$\mathbf{K}_{pj} + 2(j + 1)\mathbf{K}_f = \mathbf{K}_{dj}. \qquad (5)$$

Substitutions in Eqs. (3)–(5) result in phase-matching conditions valid for all processes:

$$(2j + 1)(\mathbf{k}_\alpha - \mathbf{k}_\beta) = \mathbf{k}_{\delta j} - \mathbf{k}_{\gamma j}, \qquad (6)$$

with the relation between scattering and pump angles:

$$\sin\theta_{sj} = (2j + 1)\sin\theta_p. \qquad (7)$$

Equation (7) fits experimental data with a great accuracy (see solid lines in Fig. 2). According to Eq. (7), the highest possible number of scattering lines is defined by the pump
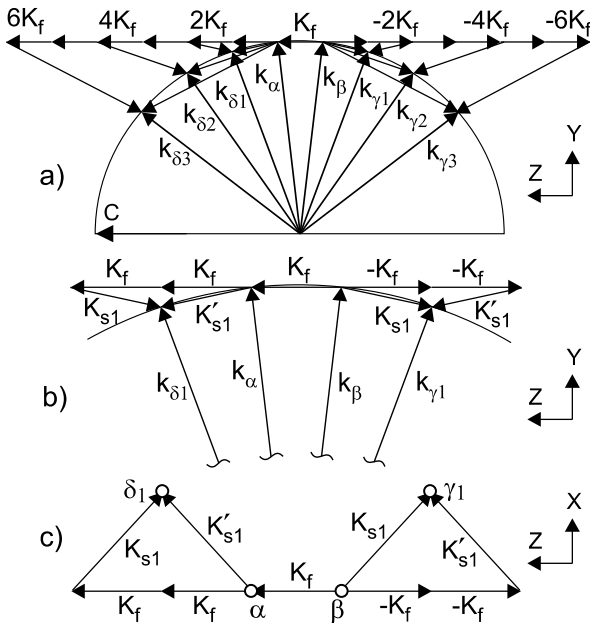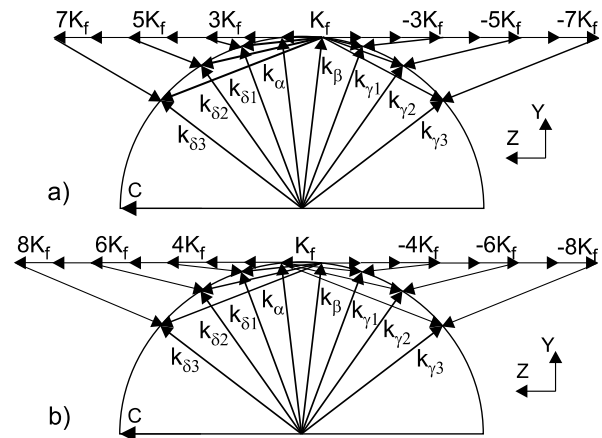

FIG. 4. Phase matching diagrams of 4WM processes described by Eq. (3): The general view in the plane of incidence for $j = 3$ (a), and the large-scaled view for $j = 1$ (lines γ_1 and δ_1) in the plane of incidence (b) and in the viewing plane (c).

FIG. 5. Phase matching diagrams of 4WM processes described by Eq. (4) (a) and Eq. (5) (b) shown in the plane of incidence.

angle and equals $j_{max} = \text{Int}[0.5(1/\sin\theta_p - 1)]$: no lines at all are allowed at $\theta_p \gtrsim 19.5°$, while at $\theta_p = 3°$ one can expect up to 9 pairs of lines. However, the actual number of lines appearing in the experiment is limited by the 4WM efficiency which strongly decreases with increasing line index j, because the number of vectors $\mathbf{K}_f$, necessary to enclose the phase-matching diagram, also increases with j. The 4WM efficiency also depends on the strength of the fundamental grating, and therefore the scattering intensity should exhibit a strong dependence on m_p (see Fig. 3). The substantial contraction of the $I_{\gamma 1}$ curve shows that the number of vectors $\mathbf{K}_f$ involved in the 4WM is more than one. The geometry of new 4WM processes should result in additional interesting effects of interference and cascading of 4WM processes. The interference effect is obvious from the fact that different 4WM processes shown on Figs. 4 and 5 yield the same scattering pattern. This should result in either summation or subtraction of their exponential increments Γ, if different 4WM processes are in phase or not. A cascading effect describes 4WM of pairs of scattering waves with different indices j. For instance, pairs $\delta_1 - \delta_2$ and $\gamma_1 - \gamma_2$ record gratings mutually coupled by the vector $2\mathbf{K}_f$, that causes additional parametric mixing of scattered waves.

The dominating space charge transport mechanism in SBN is diffusion of thermalized photoelectrons, causing a $\pi/2$ shift of the recorded photorefractive gratings with respect to the initial interference patterns. Such a spatial shift allows additional light amplification by two-wave coupling [6] in the $-\mathbf{c}$ direction in SBN, which usually leads to the development of spatially asymmetric wide-angle scattering [12] seen in Fig. 1. The direct pump-seed coupling also results in an additional enhancement of γ lines and a depletion of δ lines.

If one compares Eq. (2) with Eq. (6), one can classify the processes shown in Figs. 4 and 5 as B processes with phase-matching conditions extended by the matching vector $\mathbf{K}_B$, which in our particular case is proportional to the fundamental vector. For an arbitrary grating $\mathbf{K}_B$, unified phase-matching conditions for B processes can be written as

$$\mathbf{k}_\alpha - \mathbf{k}_\beta + j\mathbf{K}_B = \mathbf{k}_\delta - \mathbf{k}_\gamma. \qquad (8)$$

For $j = 0$, Eq. (8) is reduced to Eq. (2) ($\mathbf{K_s} = \pm\mathbf{K'_s}$), while for $j \neq 0$ it describes new scattering processes not included in the classic model. From symmetry considerations, $\mathbf{K}_B \parallel (\mathbf{k}_\alpha - \mathbf{k}_\beta)$. When evaluating the efficiency of parametric mixing, one should account phases of waves and gratings involved in the process that can depend on the parity of the index j. An absence of lines induced by the parametric mixing with $\mathbf{K}_B = \mathbf{K}_f$ indicates that in our case only processes with even numbers of the fundamental grating $\mathbf{K}_f$ are efficient enough.

Similarly to Eq. (8), unified phase-matching conditions for A processes can be written as

$$\mathbf{k}_\alpha + \mathbf{k}_\beta + j\mathbf{K}_A = \mathbf{k}_\delta + \mathbf{k}_\gamma. \qquad (9)$$

Unlike the grating $\mathbf{K}_B$ in B processes, the matching grating $\mathbf{K}_A$ is expected to be parallel to $\mathbf{k}_\alpha + \mathbf{k}_\beta$. Equations (8) and (9) are general expressions for phase-matching conditions which are able to cover all known and new types of parametric scattering. The angle-selective scattering recently discovered in bulk periodically poled LiNbO$_3$ (PPLN) [13] can be classified as new A processes: phase-matching conditions describing pairs of anomalous scattering spots in PPLN are easily reduced to Eq. (9) if the ferroelectric domain grating $\mathbf{G}$ is regarded as the grating $\mathbf{K}_A$.

In summary, a new parametric scattering has been found in SBN:Cr, which consists of series of polarization-isotropic light cones. It is explained by a new 4WM model, where especially fundamental gratings recorded by the pump beams are taken into account. Thereby, generalized phase-matching conditions are proposed, which are valid for all known types of parametric scattering processes. The study of the new scattering phenomenon is important for a better understanding of processes of complex multiwave mixing in nonlinear media including effects of interference and cascading of elementary 4WM processes. The new scattering can be useful for applications in mirrorless photorefractive self-oscillation and in optical image processing. Taking into account recent investigations of light-induced scattering as a function of the polar structure in SBN [14], parametric scattering is a good candidate for a detailed study of such fundamental questions as primary scattering centers in photorefractive crystals and in some cases (such as SBN) even for the study of the polar structure.

[1] E. K. Kirilenko, Sov. J. Quantum Electron. **19**, 930 (1989).
[2] T. N. Smirnova and E. A. Tikhonov, Sov. J. Quantum Electron. **9**, 93 (1979).
[3] M. Imlau *et al.*, Appl. Phys. Lett. **75**, 16 (1999).
[4] I. C. Khoo and Y. Liang, Phys. Rev. E **62**, 6722 (2000).
[5] B. I. Sturman, S. G. Odoulov, and M. Yu. Goulkov, Phys. Rep. **275**, 197 (1996).
[6] P. Yeh, *Introduction to Photorefractive Nonlinear Optics* (John Wiley and Sons, Inc., New York, 1993).
[7] J. Neumann *et al.*, Opt. Commun. **146**, 220 (1998).
[8] P. P. Banerjee *et al.*, Opt. Laser Technol. **28**, 89 (1996).
[9] R. A. Rupp, J. Seglins, and U. van Olfen, Phys. Status Solidi (b) **168**, 445 (1991).
[10] S. G. Odoulov, Ferroelectrics **92**, 213 (1989).
[11] L. I. Ivleva *et al.*, Opt. Mater. **4**, 168 (1995).
[12] V. Voronov *et al.*, Sov. J. Quantum Electron. **10**, 1346 (1980).
[13] M. Goul'kov *et al.*, Phys. Rev. Lett. **86**, 4021 (2001).
[14] M. Goulkov *et al.*, J. Appl. Phys. **94**, 4763 (2003).